Phytoassisted synthesis of biogenic silver nanoparticles using *Vernonia amygdalina* leaf extract: characterization, antibacterial, anti-inflammatory, and acute toxicity profile

Fonye Nyuyfoni Gildas[1#], Nkana Blondeau Parfait[2#], Vandi Deli[2], Belle Ebanda Kedi Philippe[2], Ntoumba Agnes Antoinette[3], Nanga Chick Christian[4], Chimi Tchatchouang Geordamie[5], Djuidje Annie Guilaine[2], Tako Djimefo Alex Kevin[3], Evouna Ines Danielle Madeleine[6], Essombe Malolo Fanny-Aimee[2], Kang Eha-Kang Costly[2], Kwati Leonard[7], Gilbert Njowir Ndzeidze[8], Paboudam Gbambie Awawou[1], Eya'ane Meva Francois[2,*]

[1]*Department of Inorganic Chemistry, Faculty of Science, University of Yaoundé, Yaoundé, Cameroon*
[2]*Department of Pharmaceutical Sciences, Faculty of Medicine and Pharmaceutical Sciences, University of Douala, Douala, Cameroon*
[3]*Department of Biology of Animal Organisms, Faculty of Sciences, University of Douala, Douala, Cameroon*
[4]*Department of Materials and Life Sciences, Faculty of Science and Technology, Sophia University, Chiyoda-ku, Tokyo, Japan*
[5]*Department of Chemistry, University of Douala, Cameroon*
[6]*Clinical Biology, Faculty of Medicine and Pharmaceutical Sciences, University of Douala, Douala, Cameroon*
[7]*International institute for Carbon-Neutral Energy Research (WPI-I2CNER), Kyushu University, 744 Motoka, Nishi-ku, Fukuoka 819-0395, Japan.*
[8]*Department of Chemistry, Faculty of Sciences, Marquette University, Milwaukee, Wisconsin, United States of America.*

Corresponding author: Francois Eya'ane Meva, mevae@daad-alumni.de
Contribute equally to the research

ABSTRACT

The increasing rate of antimicrobial resistance and pathological consequences associated with long-term use of available anti-inflammatory drugs justifies the urgent need to discover and rationally design new effective antimicrobial and anti-inflammatory drugs. This study reports the antibacterial, anti-inflammatory, and acute toxicity profile of *Vernonia amygdalina* leaf extract-mediated silver nanoparticles (VA-AgNPs). The VA-AgNPs were synthesized by mixing Ag^+ ions with aqueous leaf extract from *Vernonia amygdalina* and then characterized using UV-visible spectrophotometry (UV-Vis), X-ray diffraction (XRD), and scanning electron

microscopy (SEM). An antibacterial study on *Escherichia coli* strains, carrageenan-induced rat paw edema, and oral acute toxicity assays were performed. The change in color from light brown to dark brown indicated the formation of VA-AgNPS which was further confirmed by the surface plasmon resonance picked between 400 and 450 nm on the UV-Vis spectrum. Synthetic stability studies revealed an increase in VA-AgNP formation at basic pH and with increasing reactant quantities. The X-ray pattern showed nanocrystalline particles of Ag and AgCl of 13, and 18 nm mean sizes, respectively. SEM images depicted aggregates of spherical shape. The synthesized VA-AgNPs inhibited *Escherichia coli* growth with a minimum inhibition concentration of 0.125 mg/mL and rat paw edema with a maximum inhibition percentage of 96% at a dose of 0.4 mg/kg body weight. The oral administration of VA-AgNPs was associated with no toxicity sign, supporting their use for the development of new effective antibacterial and anti-inflammatory drugs.

Keywords: Biosynthesis, silver nanoparticles, *Vernonia amygdalina*, antimicrobial, anti-inflammatory, acute toxicity

INTRODUCTION

Recent scientific and technological progress has led to the development of materials with at least one dimension in the nanoscale range, known as nanomaterials. At this length scale, certain novel size-related properties develop, and the material exhibits completely new or improved properties relative to the bulk material that they are made up of [1]. Although nanomaterials exist from ancient times having natural or synthetic origin, they have recently attracted more attention from researchers, because they found applications in various fields including the biomedical area, cosmetics, pharmaceutics, solar systems, energy storage, and other. Metal nanoparticles are an attractive choice because of their ability to control their composition, shape, structure, encapsulation, assembly, and their optical properties during synthesis. Furthermore, their special surface properties such as plasmon excitation give them a high applicability as a biosensor, biomarker, catalyst, electronic devices, delivery of therapeutic agents, hyperthermal treatment for cancer (Kumar et al., 2013). Bacterial infections are a global burden in public health, and the increasing rate of antimicrobial resistance might lead to potentially devastating consequences. Numerous studies focused on the development of nanoparticles with antibacterial potential as new therapeutic agents have presented many advantages compared to conventional methods. The rich diversity of its resources is explored for the synthesis of bionanomaterials [2]. In fact, now-a-days, colloidal silver nanoparticles

have been used as antimicrobial agents, wound dressing material, bone and tooth cement, and water purifiers as well [3]. The most common methods for preparing most of these nanoparticles are wet-chemical techniques, which are low-cost and high-volume. The chemical synthesis of silver nanoparticles employs chemical reducing agents to convert Ag^+ ions to Ag^0. One of the widely used chemical reducing agent is sodium borohydride. However, the need for toxic solvents and the contamination from this chemical used in nanoparticle production limit its potential use in biomedical applications. This process involves undesired hazardous chemicals, and the biocompatibility of the resulting AgNPs is too low for the application in biological systems. Recent efforts have focused on developing new green chemistry methods for the synthesis of silver nanoparticles with the advantage of using natural products and avoiding toxic reducing agents, organic solvents, and wasteful purifications with high residual cytotoxicity [4]. Molecules produced by living organisms, such as bacteria, fungi, or plants, can replace the reducing and capping agents to produce nanoparticles [3].

Vernonia amygdalina, commonly known as bitter leaf, is a shrub that grows up to 2-5 meters high in African countries, including Cameroon, Zimbabwe, and Nigeria [5]. It belongs to the Asteraceae family, with a petiolate leaf of about 6 mm in diameter, and elliptical shape [6]. The is traditionally used against amoebic dysentery, and gastrointestinal disorders [7]. The biologically active compounds of *Vernonia amygdalina* are saponins and alkaloids, terpenes, steroids, coumarins, flavonoids, phenolic acids, lignans, xanthones and anthraquinone, edotides and sesquiterpenes[8]. In this study, the viability against E. coli strain of the optimized AgNPs as well as their anti-inflammatory activity and acute toxicity will be presented considering the potential therapeutic considerations.

MATERIALS AND METHODS

Selection of Bacteria.

Escherichia coli strains were isolated from urine samples in the bacteriology unit, of the General Hospital laboratory, Yaoundé, Cameroon.

Plant Extract.

Fresh bitter leaves *(Vernonia amygdalina)* were harvested on 14 July 2020, at Logpom, Littoral region, Cameroon and authenticated at the National Herbarium of Cameroon, in comparison with a voucher specimen previously deposited (N°32875 HNC). *The leaves of V. amygdalina* were surface cleaned with running tap water followed by deionized water to remove all the dust and visible unwanted visible particles. Aqueous extract of *V. amygdalina* was prepared by

boiling 25g of finely cut leaves in 250 mL of deionized water for 5 min at 80 °C and stirred for 5 min using a hot plate equipped with magnetic stirrer. The extract was filtered through Whatman No. 1 filter paper and cotton to remove particulate matter, brown solution gotten was stored at 4 °C for further use, being usable for 1 week due to the gradual loss of plant extract viability for prolonged storage.

Figure 1: *Vernonia amygdalina*

***Synthesis of Silver Nanoparticles*.**

Silver nitrate ($AgNO_3$) was obtained from Sigma-Aldrich chemicals Germany. Deionized water was used throughout the reactions. All glassware was washed with dilute nitric acid (HNO_3) and deionized water and then dried in a warm air oven. Different experiments were carried out for three extract quantities named (5 mL, 10 mL, and 15 mL), using 50 mL of different concentrations of $AgNO_3$ (10^{-3} M, 10^{-2} M, and 10^{-1} M) at room temperature and pressure. The resulting solutions were 1 min hand shaken and wrapped with aluminum foil paper and then incubated in the dark to minimize photoactivation of silver nitrate. The reactions were made under static conditions. The color of the solutions changed from initial light brown (which is the color of the *Vernonia amygdalina* leaf extract) to orange in 5 minutes. The first hour of reaction was monitored by ultra-violet visible spectroscopy of 2.5 mL of the reaction suspension using a UV-Vis Uviline 9100 spectrophotometer operating at 1nm resolution with optical length of 10 mm. Concentrations were determined by centrifugation after 24 hours of incubation. UV-Vis analysis of the reaction mixture was observed for a period of 300 seconds. Powder X-ray diffraction measurements were carried out using a Rigaku Miniflex II instrument by preparing a thin film of the silver-organic nanopowder on a silicium substrate.

Determination of the Minimum Inhibitory Concentration (MIC) and the Minimum Bactericide Concentration (MBC).

For the evaluation of antimicrobial activity, a multidrug resistant clinical isolate *Escherichia coli* strain will be tested against the suspensions of AgNPs. This method assesses the sensitivity of bacteria and yeasts to different samples according to the microdilution described in ISO standard ISO 20776-1, 2006 and amended by the Antibiotic Committee of the French Society of Microbiology (CA-SFM / EUCAST 2019). The microdilution in liquid medium of EUCAST 2019 was used with some modifications [9]. The principle consists of diluting the suspensions of AgNPs in a liquid culture medium and inoculating this medium with microbial strains to be tested. A volume of 1 mL of the sample at a concentration of 10 mg / mL was added to 4 mL of Muller Hinton Broth (MHB) culture medium; A 96-well microplate was used in which 100 µL of the previous mixture is distributed in the wells of column 1 in triplicate; 50 µL of the medium used previously is also distributed in the wells 2 to 12 in triplicate as well;

A successive geometric progression dilution of a ratio of 2 of the sample is carried out from well 1 in the wells 2 to 10 and the excess volume in the wells 10 is removed; the 10th, 11th and 12th wells consisted of the negative control (sample + culture medium), the positive control (inoculum + culture medium) and the sterility control (culture medium only) respectively; 50 µL of a preparation consisting of 130 µL of inoculum at 0.5 mL Mc Farland and 19.85 mL of culture medium are added to each wells. The concentration range of the samples in the reaction medium was 1; 0.5; 0.25; 0.125; 0.0625; 0.0312; 0.0156; 0.0078; 0.0039; 0.0019 mg/mL. While that of microorganisms is substantially $5x10^5$ CFU/mL for bacteria; Microplates were incubated at 35°C for 18-24 hours and the MIC was considered the smallest sample concentration for which no growth was observed;

In bacteria, tetrazolium chloride was used as a color indicator; The MBC was determined by transplanting 50 µL of suspension from each well where no shoots were observed in the corresponding 50µL crop medium. This was the smallest concentration for which no shoots were observed after transplanting.

From these reports the bacteriostatic or bactericidal nature of a substance was confirmed. When these ratios are greater than or equal to 4, the substance is said to be bacteriostatic; if these ratios are less than 4, the substance is bactericidal. If they are equal to 1, then it is said to be "absolute bactericidal".

Evaluation of anti-inflammatory activities

Animals and ethics

For this study Wistar albinos' rats of 8 weeks old, weighing 130 - 150 g, housed in a standard polypropylene cage at room temperature (24 °C ± 2 °C) and relative humidity in the light and dark cycle (from 6 am to 6 pm) were used. They were obtained from the rearing facility, Department of Pharmaceutical Sciences, Faculty of Medicine and Pharmaceutical Science, University of Douala. They were fed with standard pellet food and tap water ad libitum during 1 week of acclimatization. All experiments were carried out according to the protocol approved by the Institutional Ethics Committee of the University of Douala (protocol approval number CEI-UDo/2617/05/2017/T).

Carrageenan-induced rat paw edema method

The anti-inflammatory activity of silver nanoparticles was evaluated on a carrageenan-induced model of rat paw edema as described by Winter et al. [10]. The experimental animals were randomly divided into five groups (n=6). Group I served as a control receiving the inflammatory inducing agent diclofenac. Group II served as standard, and groups III, IV, and V served to test. Acute inflammation was induced by a single subplantar injection of 0.1 mL of carrageenan (1% carrageenan suspended in 0.9% NaCl) into the right hind paw of the rats 1 hour after administration (per os) of silver nanoparticles at doses of 100, 200, and 400 µg/kg for the test groups, indomethacin (10 mg/ kg) for the standard group, or distilled water (10 mL/kg) for the control group. Diameters were measured using a digital caliper (Hardened Stainless) immediately before and 30 minutes, 1 hour, 2 hours, 3 hours, 4 hours, and 5 hours after carrageenan injection. The edema was expressed as the increase in paw volume, and the percentage of inhibition of edema was expressed as the reduction in volume with respect to the control group using Equation 1:

$$\% \text{ inhibition} = \frac{(\boldsymbol{Dt-Do})\boldsymbol{control} - (\boldsymbol{Dt-Do})\boldsymbol{treatment}}{(\boldsymbol{Dt-Do})\boldsymbol{control}} \times 100 \quad [11]. \quad (1)$$

Dt: mean diameter for each group after treatment,

Do: average diameter for each group before treatment.

Assessment of acute toxicity on rats of the Wistar strain.

The AgNPs toxicity test was performed according to the OECD guideline 425. These were the limit tests at the dose of 2000 mg / kg in rats of the Wistar strain. Batches of 3 female rats were made for each sample tested, and one batch represented the control group in which distilled water was administered [12].

The rats were evenly distributed in batches with masses between 120 and 180 g before being subjected to a non-water fast for 12 hours prior to sample administration.

The administration of the samples and of distilled water was performed in one dose by gavage using a gastric tube after calculating the concentrations and volumes to be administered according to formula 2:

$$C = \frac{mxD}{V} \qquad (2)$$

C: Concentration;

D: Dose;

m: Mass of the rat;

V: volume of solution to be administered. (1 mL for a 100 g rat)

Clinical parameters were monitored at regular time intervals during the hours after gavage and the resumption of the feeding of rats took place 4 hours after administration. At the same time, weight monitoring of rats was done every day, and their growth rate was calculated according to the following formula 3:

Growth rate = (mass of rat on day x- mass of rat on day 0)/(mass of rat on day 0) x 100 (3)

14 days later, the rats were anesthetized with a ketamine solution and their blood was drawn after incision of their carotid artery for analysis of biochemical parameters. Some organs such as the liver, kidneys, lungs, heart, and spleen have been removed using surgical scalpel blades, forceps, and scissors.

RESULTS AND DISCUSSION

Ultraviolet Visible Spectroscopy.

The absorption spectra of the synthesized silver nanoparticles were plotted against water to study the formation and stability of Ag nanoparticles. The color change of the plant extract and silver ion solution mixture is first seen through visual monitoring. The color of silver nitrate, *V. amygdalina* leaf extract, and silver nanoparticles solution is shown on Figure 2. The progress of the surface Plasmon absorbance bands during the first hour when mixing 50 mL of $AgNO_3$ 10^{-3} M with 10 mL of extract is shown in Figure 2. The solution color changed within seconds to pale yellow, and then brown, due to the formation of plasmons at the colloid surface, indicating the synthesis of silver nanoparticles. The same sharp surface plasmon resonance absorbance band has been obtained with different extract concentrations (5, 10, 15mL) at 10^{-3} M $AgNO_3$. Then, 5 mL of extract is enough to completely reduce 50 mL of silver ion at a concentration of 10^{-3} M (Fig. 2).

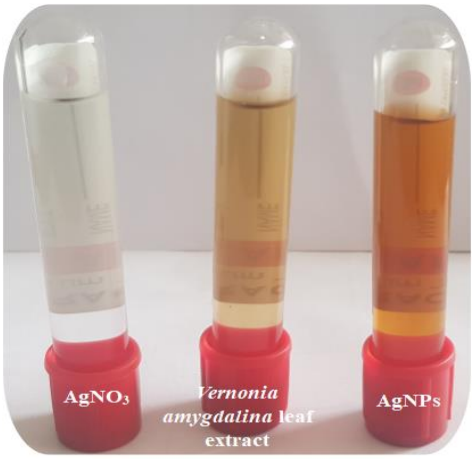

Figure 2: Silver nitrate, *Vernonia amygdalina* leaf extract and AgNPs

Plasmon resonance absorbance increases when a 10^{-2} M $AgNO_3$ solution is used with different extract concentrations, then more silver ion is available for reduction. At 10^{-1} M concentration of silver ions with different *V. amygdalina* extract concentrations, the nanoparticles aggregate because of the deficiency of leaf extract molecules to act as capping agents. The barrier potential developed because of the competition between the weak Van der Waals forces of attraction and electrostatic repulsion is broken [13]. As postulated by Mie's theory, spherical nanoparticles result in a single surface plasmon resonance (SPR) band in the absorption spectra. On the other hand, anisotropic particles provide two or more SPR bands, depending on the shape [14]. In the present study, reaction mixtures confirm single SPR bands, disclosing the spherical shape of AgNPs that tend to become anisotropic with time. The plant leaf extract of *V. amygdalina* acts as a reductant as well as a stabilizer for the silver nanoparticles. The sharp surface Plasmon resonance band increases with silver ion concentration, as observed for the *Megaphrynium macrostarchyum* leaf extract [15].

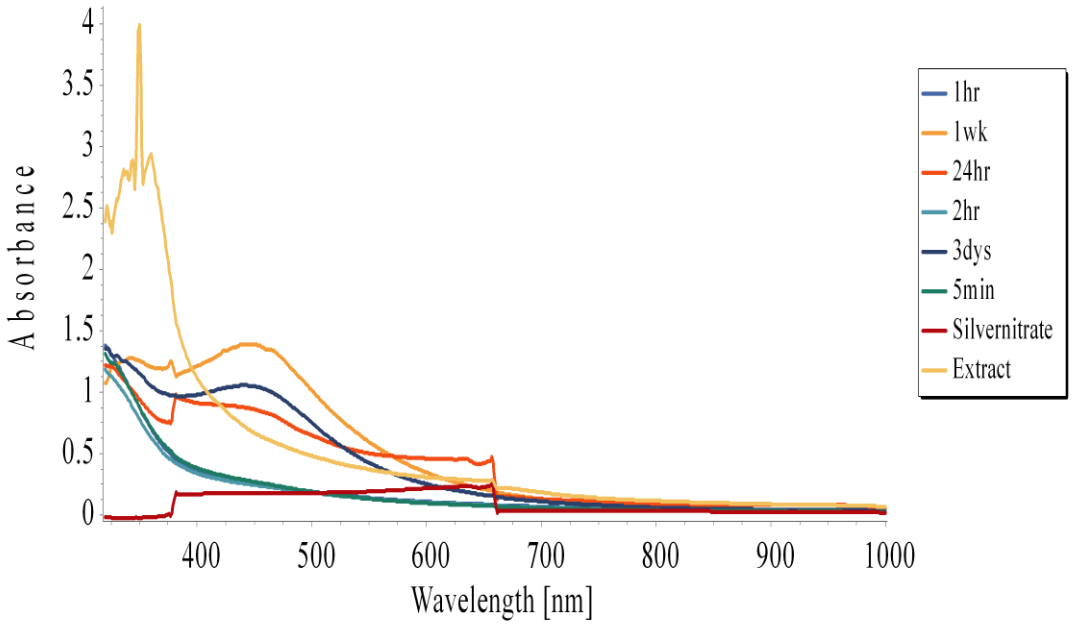

***Figure 3: UV/Vis spectra of AgNPs with respect** to*

Figure 3 presents time-recorded spectra between 5 minutes and 1 week for a mixture of 3 mL of the aqueous extract and 10 mL of silver nitrate solution of 1 mM. This result shows a wide range of AgNPs SPR from the 5th minute with a SPR band between 350 and 550 nm. The absorption intensity of the SPR band increases over time and starts forming a plateau from 24 hours with an absorption intensity of 0.9 until it reaches its highest plateau in one week with an absorption intensity of 1.5.

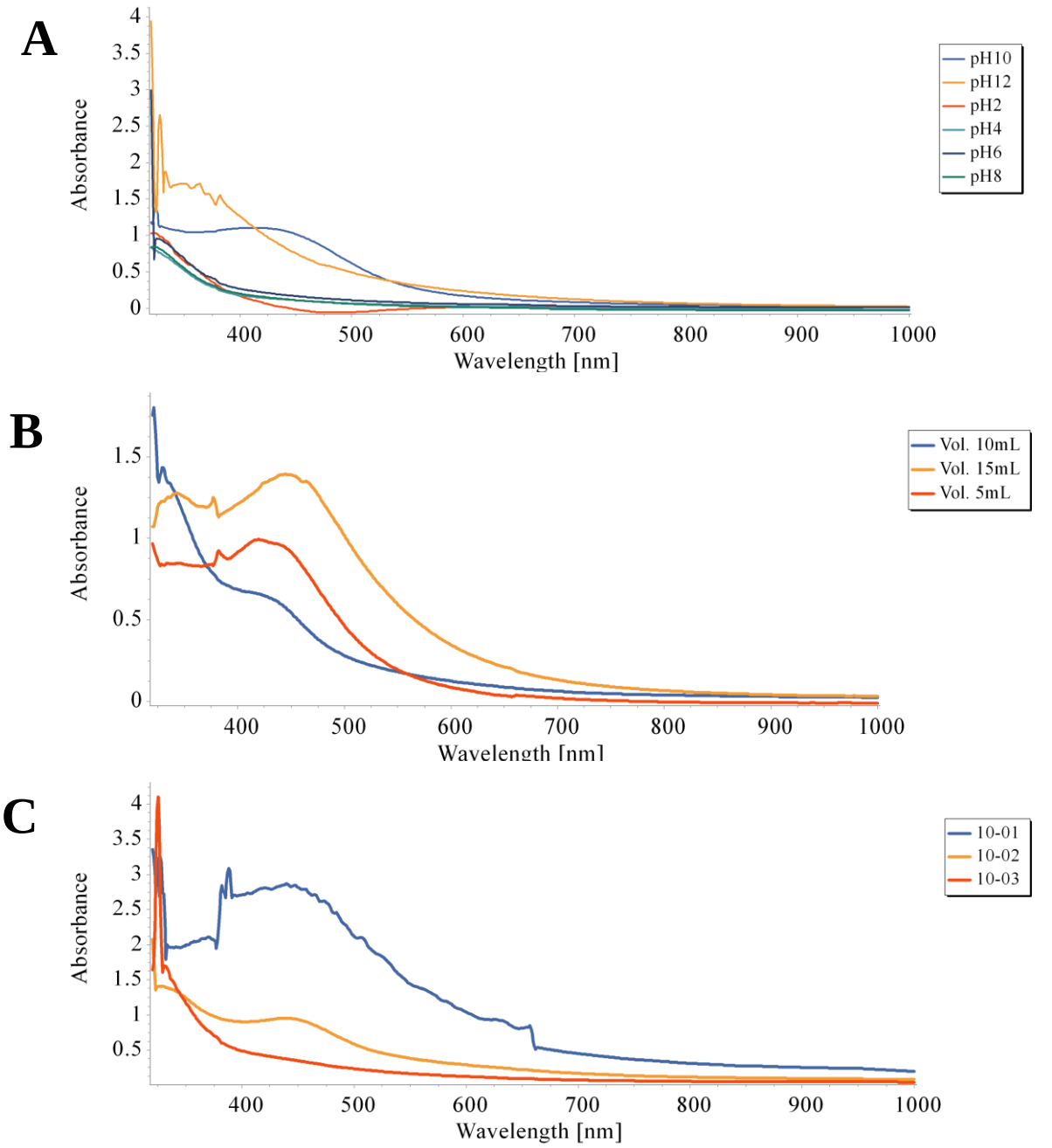

Figure 4: A, B and C Increase in the intensity of the SPR band with an increase in pH, extract volume and silver nitrate concentration, respectively.

The maximum absorbance of AgNPs using *V. amygdalina* are in the range 400 - 450 nm due to the surface plasmon resonance of AgNPs [16].

The conduction electrons undergo oscillation due to the strong interaction of light with the silver nanoparticles [17]. As the concentration of the *V. amygdalina* extract increases together with the absorption peak but tends to be polydisperse. A sharp narrow-shaped SPR band was observed, indicating the formation of a spherical and homogeneous distribution of the AgNPs.

The UV-Vis spectra also revealed that the formation of AgNPs occurred rapidly within a few minutes, indicating that *V. amygdalina* speeds up the biosynthesis of silver nanoparticles. This rapid reduction was observed for carob leaf extract with a 2 min reduction [18].

The reaction between Ag^+ and the reducing material in the extract was followed for 1 week and the UV-Vis spectra of AgNPs was recorded as a function of time after the addition of different amounts of *V. amygdalina* leaf extract. The reduction, as well as nucleation and growing size of nanoparticles, increases from 24 h to 1 week, but polydispersions occur. The reaction time resulted in a gradual increase in absorbance bands. The color intensity of the solution changes from light yellow to deep brown at the end of the reaction because of increasing amount of AgNPs and the aggregation.

Effect of pH

The UV-Vis measurements of the pH variation during the formation of silver nanoparticles from 2 to 12 are shown in Figure 4. The variation of color is shown in Fig. 5. The absorbance increases with the pH, which can be due to the increase in production of colloidal silver nanoparticles and reduction rate. Absorbance does not decrease at pH higher than 8 as observed for *Megaphrynium macrostachyum* leaf extract [15].

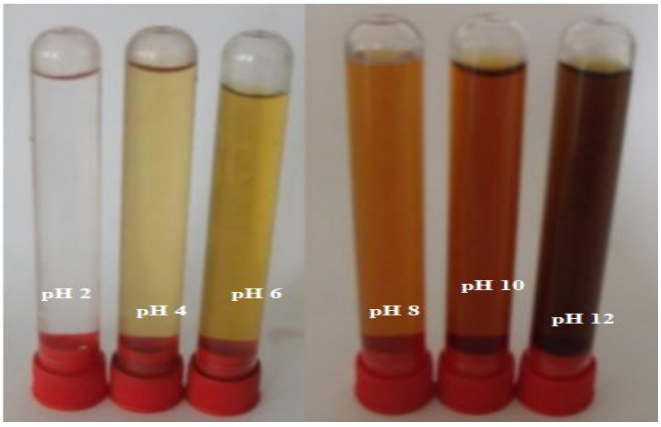

Figure 5: *Influence of pH*

Furthermore, it is observed that the brown color of the nanoparticles appeared shortly after mixing $AgNO_3$ with the extract at pH 4-12. As observed in the bark extract of *Pinus eldaria,* pH affects the amount of nanoparticle production and its stability and is a critical factor in controlling the size and morphology of nanoparticles [19]. Again, the pH influenced the rate of the reduction reaction. The reaction mixture turned brown when silver was reduced, and the reaction mixture coloring accelerated with increasing pH. At pH 10, the sharp surface Plasmon

resonance band indicates that a monodisperse suspension occurs. Previous investigations showed that the size and shape of biosynthesized nanoparticles could be manipulated by varying the pH of reaction mixtures [20]. A major influence of the pH of the reaction is its ability to change the electrical charges of biomolecules that could affect their capping and stabilizing abilities, and then the growth of the nanoparticles [20]. Then, the high pH environment facilitated the reduction and stabilization capacity of antioxidants in the *Vernonia amygdalina* leaf extract, a situation found for the olive leaf extract. The number of nuclei increases with increasing pH due to promoted reactivity of the V. amygdalina leaf extract reductants.

X-ray diffraction.

X-ray diffractometry was performed on AgNPs. It revealed the nanocrystalline structure of the formed nanoparticles. The diffractogram presented in Figure 5, shows 2Θ angles ranging from 20 to 60 degrees, emerging a series of crystalline plane with the presence of peaks at 27.7°; 32.1°;38.1°; 44.2° 46.2°; 54.7° and 57.3°.

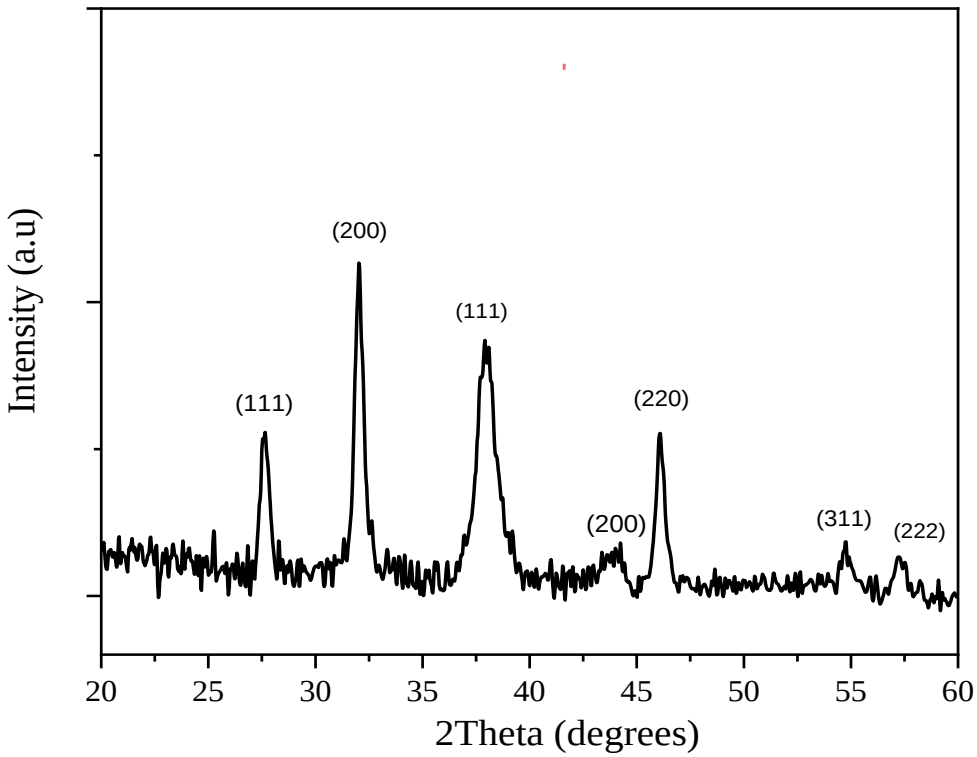

Figure 5 XRD Spectrum of AgNPs

The average crystallite size of the synthesized NP was determined using the Debye-Scherrer equation:

$$D = \frac{0.94\lambda}{\beta \cos(\theta)} \quad (3)$$

Where D is crystallite size (nm); λ is X-ray wavelength (λ = 1.5406 Å); β is Full width at Half Maximum (FWHM) of the diffraction peaks measured in radians; θ is the Bragg diffraction angle. No other characteristic peaks were found in the XRD spectra, indicating the high purity of the as-prepared Ag and AgCl nanoparticles. To calculate the average crystalline particle size of the synthesized Ag and AgCl nanoparticles, we preferred intense peaks of Ag and AgCl. 2θ values of 38.052° and 44.249° that can be indexed to the (111) and (200) planes of the face-centered cubic (FCC) structure, respectively (JCPDS file: 65-2871). The XRD pattern also showed the presence of the cubic phase of silver chloride at 2θ values of 27.683°; 32.120°;46.173°; 54.748° and 57.299° corresponding to the planes (111, 200, 220, 311) and (222), respectively (JCPDS file: 31-12380) [10]. The calculated average crystalline particle size was 13 and 18 nm for silver and silver chloride, respectively.

SEM images and microanalysis.

Figure 6 shows the surface morphology of the green AgNPs synthesized. The images give a spherical shape for all samples with a cluster of aggregation. The aggregation was gradually reduced as the concentrations increased.

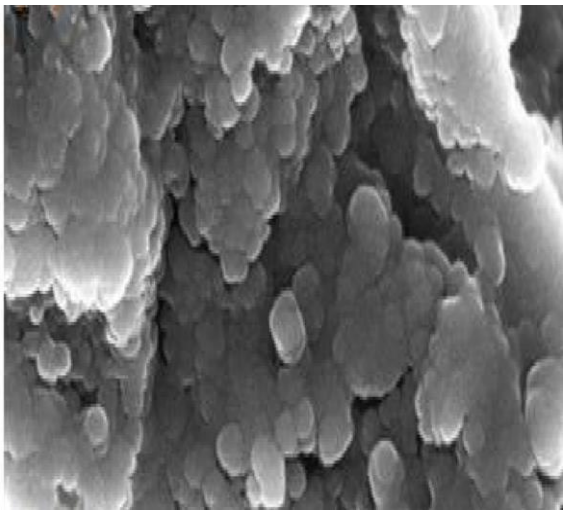

Figure 6 SEM images of AgNPs

Microbiological Assays:

The resistance of human pathogens to the commercially available antimicrobial agents and antibiotics has raised the need to explore new natural and inorganic substitutes to overcome the problem [21]. Le et al. [22] demonstrated that Ag nanoparticles are attached to the cell surface of E. coli and then penetrate the cell, destroy the cell cytoplasm, and kill the organism. Le et al. [22] also found that Ag nanoparticles significantly increase cell permeability and affect proper transport through the plasma membrane. It appears that sulfur and phosphorus from proteins or enzymes or phosphorus moiety of DNA of the bacterial system may be affected by AgNPs that lead to the inhibition of the enzyme system of the organism [23].

Microbiology control sample

AgNPs and the aqueous extract have been subjected to microbiological control to ensure that they are not contaminated with germs that may grow on culture media used for antimicrobial testing. Table 1 represents observations of culture media impregnated with samples after 48 hours of incubation.

Table 1 Microbiological control of samples

Samples	**Muller Hinton**	**Sabouraud**	**Chapman**	**Hektoen**	**MBE**
AgNPs	A	A	A	A	A
Aqueous Extract	A	A	A	A	A

A : Lack of shoots

After seeding samples in the Muller Hinton, sabouraud, chapman, hektoen, and MBE mediums, no shoots were observed after 48 hours of incubation.

The minimum inhibitory and bactericidal concentrations.

Evaluation of the antimicrobial activity of the synthesized sample in the multiresistant *E. coli* strain gave values of MIC and MBC, which we compared with the references (CIPRO and aqueous extract). These values are recorded in Table 2.

Table 2 MIC and MBC of the sample tested on E. coli multiresistant strain compared to Ciprofloxacin.

Microbial strain	***Escherichia coli***

	MIC (mg / mL)	MBC (mg / mL)	MBC/MIC
Aqueous Extract	1,000	> 1,000	/
AgNPs	0,125 ± 0,000	0,125 ± 0,000	1,000 #
CIPRO	0,004 ± 0,000	0,004 ± 0,000	1,000 #
Positive control	-		
Negative control	+		
Sterility control medium	-		

No shoot (-); The presence of a shoot (+); Bactericidal (#)

The sample has a much higher MIC than ciprofloxacin on the multiresistant germ tested (Table 2). Evaluation of the MBC of the synthesized AgNPs shows that they are bactericidal against multiresistant *E. coli*.

The determination of the AgNPs MIC was carried out in comparison with that of the aqueous extract and a reference. These nanoelements demonstrated interesting antibacterial activities with respect to the multiresistant strain, although that was low compared to the activity of the reference. These activities are related to the possibility of releasing the silver ions directly into the microbial cell that will be able to act on various sites. Synthesized nanoparticles are covered with molecules from the extract that may also have intrinsic antimicrobial properties [24]. Therefore, AgNPs would also play a good role as a vector for delivering Ag^+ ions and molecules from the extract at their site of action.

Oral acute toxicity

Concerning acute oral toxicity, all animals treated with AgNPs-VA survived (Figure 7). This result suggests that the median lethal dose (LD_{50}) of AgNPs-VA is higher than the maximum dose administered (2000 mg/kg). According to the OECD, AgNPs-VA are not classified into the category of products at risk of acute toxicity. This result corroborates the results of Tchangou et al. (2020) who showed that nanoparticles are not toxic at a dose of 2000 mg/kg [25]. The curves do not show signs of anorexia; thus, the test models are growing well. The analysis of organ masses shows no differences between the control and test groups (Figure 8). Also, urea and creatinine do not exhibit statistically different behavior which means that the kidney of treated groups are in good health relative to the control (Figure 9). ASAT and ALAT values allow us to confirm that the liver is not damaged by the nanoparticle treatment (Figure 10).

A carrageenan-induced model of hindpaw edema in rats was used to evaluate the anti-inflammatory potential of AgNPs-VA. It is the standard experimental model of acute

inflammation used to screen the anti-inflammatory potential of various compounds in vivo. The method has a high degree of reproducibility and makes it possible to determine the mechanisms of action of the substances tested [26]. Carrageenan-induced edema is a triphasic response that involves the release of different mediators, including histamine and serotonin, in the first phase (1 hour). The second phase is mediated by the release of kinins (2 hours), and the third phase is attributed to prostaglandins and cyclooxygenase products, which last for 3 to 5 hours [27,28]. These chemicals increase vascular permeability during their production, thus promoting the accumulation of fluid in tissues that explains edema [29]. Oral pretreatment of animals with AgNPs-VA resulted in effective inhibition of the edema rate in all phases compared to the control. Maximum inhibition (96%) was obtained at a dose of 400µg/kg, 6 hours after injection. This result suggests that synthesized nanoparticles may act by inhibiting the release of histamine, serotonin, and kinins and/or by interfering with the synthesis of prostaglandin mediators as previously reported by [11]. This result is different from that of Adiukwu et al. in 2013 who demonstrated the anti-inflammatory and antipyretic activity of the leaf, root and saponin fraction of *V. amygdalina* and who had a percentage inhibition of edema of 88% at 800 mg/kg of the aqueous extract of *V. amygdalina* [30]. This shows that the AgNPs have an activity higher than that of the aqueous extract.

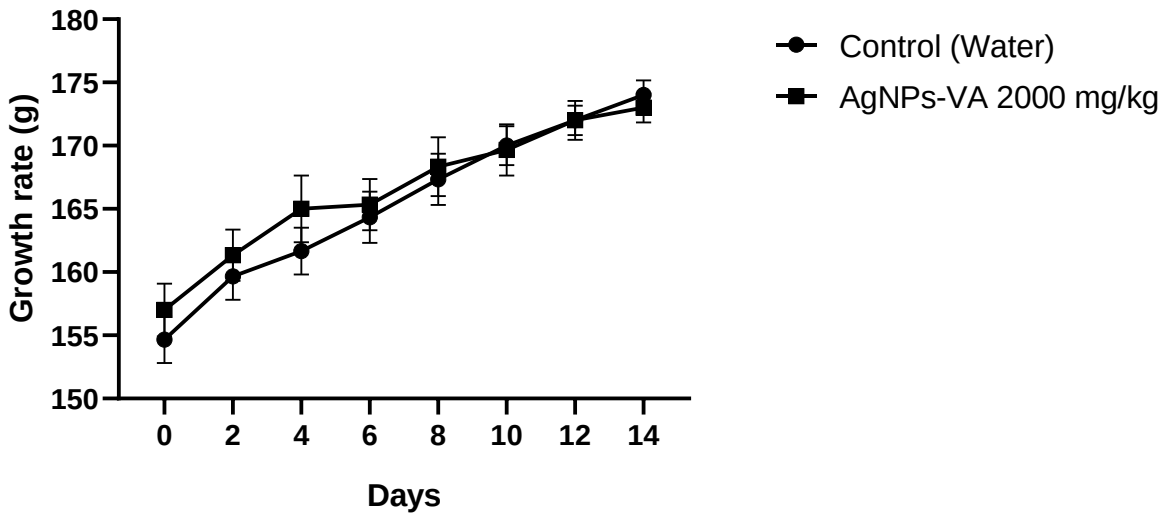

Figure 7 Growth rate of the animals during the acute toxicity assay. The mean of 3 measurement + standard error of the mean is shown. Two-way ANOVA was used for comparison. The evolution of weight reveals a normal increase in rat weight, without significant differences between the control and test batches at each day.

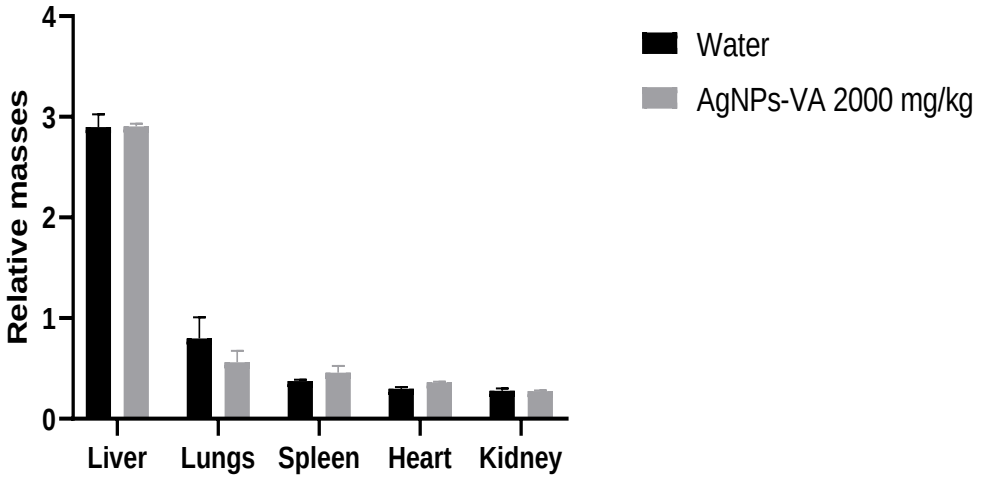

Figure 8 Comparison of the relative masses of the organs of rats tested with AgNPs compared to the control batch presenting no statistically significant differences between the test and the control group

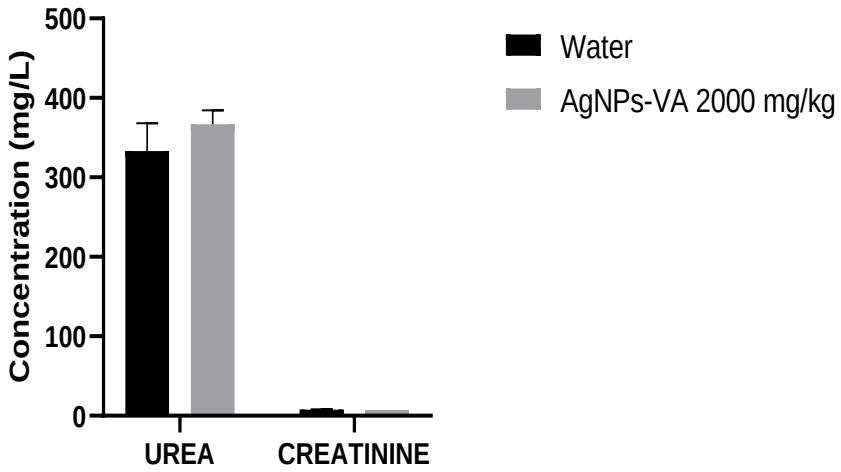

Figure 9 Comparison of creatinemia and uremia of rats subjected to the acute toxicity test for the test batch compared to the control batch without statistically significant differences between the test and the control group

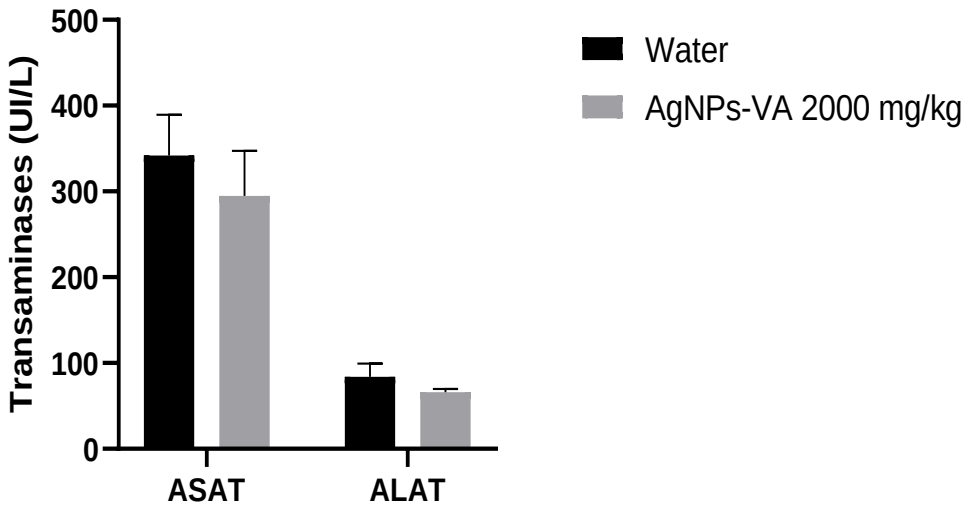

Figure 10 Serum transaminases of rats subjected to the acute toxicity test for the test and the control batch without statistically significant differences between the test and the control group

Table 3 Effect of AgNPs on rat paw.

Traitement	**Dose (mg/kg)**	**Diamètre ±SEM (cm)**						
		30 min	1 h	2 h	3 h	4 h	5 h	6 h
Control	_	0.9±0.5	0.9±0.4	0.8±0.4	1.0±0.4	0.8±0.3	0.6±0.3	0.7±0.3
Diclofénac	**10**	0.8±0.4[b] **(5)**	0.7±0.4[b] **(18)**	0.5±0.4[b] **(24)**	0.7±0.4[b] **(27)**	0.3±0.3[b] **(64)**	0.27±0.00[b] **(56)**	0.10±0.05[b] **(86)**
AgNPs-VA	**0.1**	0.9±0.2[c] **(-4)**	0.8±0.2[c] **(7)**	0.7±0.2[c] **(11)**	0.06±0.00[c] **(94)**	0.06±0.05[c] **(93)**	0.12±0.00[c] **(80)**	0.11±0.00[c] **(84)**
AgNPs-VA	**0.2**	1.0±0.2[c] **(-14)**	0.7±0.3[c] **(21)**	0.5±0.3[c] **(27)**	0.13±0.00[c] **(87)**	0.1±0.0[c] **(88)**	0.07±0.00[c] **(89)**	0.05±0.04[c] **(93)**
AgNPs-VA	**0.4**	0.8±0.2[c] **(5)**	0.7±0.3[c] **(20)**	0.5±0.3[c] **(31)**	0.3±0.2[c] **(72)**	0.18±0.00[c] **(78)**	0.05±0.00[c] **(92)**	0.03±0.00[c] **(96)**

AgNPs-VA : silver nanoparticles from *Vernonia amygdalina*

CONCLUSION

This work is focused on the spectroscopic synthetic optimizations monitoring of AgNPs formation from *Vernonia amygdalina* leaf extract. The plant extract reduces ionic silver and stabilizes their nanoparticles. An evaluation of their antimicrobial activities was conducted. Silver nanoparticles were obtained from the aqueous extract of *V. amygdalina* and silver ions and then characterized. The nanoparticles were found spherical with size 13 and 18 nm. Ag nanograin obtained possesses an antimicrobial activity against *E. coli* strain. This potential, combined to anti-inflammatory and safety, allows us to propose new therapeutic avenues to fight against microbial resistance while preserving biodiversity and the environment.

REFERENCES

1. Eya'ane Meva F, Okalla Ebongue C, Fannang S V, Segnou M L,Ntoumba A A, Belle Ebanda Kedi P, Njike Loudang R-E, Yonga Wanlao A, Mang E R, Mpondo Mpondo E A. " Natural Substances for the Synthesis of Silver Nanoparticles against *Escherichia coli*: The Case of *Megaphrynium macrostachyum* (Marantaceae), *Corchorus olitorus* (Tiliaceae), *Ricinodendron heudelotii* (Euphorbiaceae), *Gnetum bucholzianum* (Gnetaceae), and *Ipomoea batatas* (Convolvulaceae)". Journal of Nanomaterials.**2017**;(1):1-6.
2. Nahar M. K, Zakaria Z, Hashim U and Bari M. F." *Biological Synthesis of Nanosilver by Using Plants*". Advanced Materials Research.**2015**:(1)30–34.
3. Eya'ane Meva F, Segnou M. L., Ebongue C. O, Ntoumba A, Djiopang Yadou S, Aimee F. Essombe Malolo F-A, Ngah L, Massai H, Mpondo Mpondo E A" Unexplored vegetal green synthesis of silver nanoparticles : A preliminary study with *Corchorus olitorus* Linn and *Ipomea batatas* (L .) Lam". African Journal of Biotechnology. **2016**;(10):341–349.
4. Murphy M, Ting K, Zhang X, Soo C. and Zheng Z. " *Current Development of Silver Nanoparticle Preparation , Investigation , and Application in the Field of Medicine.*". Journal of Nanomaterials. **2015**;(5):34-43.
5. Aisida S. O., Ugwu K, Akpa P. A, Nwanya A. C and Nwankwo U." *Biosynthesis of silver nanoparticles using bitter leave (Veronica amygdalina) for antibacterial activities".* Surfaces and Interfaces. **2019**;(17):10-32
6. Lakshmi Y. S, Banu F. and Gopalakrishnan S. "*Green Synthesis , And Antimicrobial Activity Of Silver Nanoparticles From The Medicinal Plant Vernonia Amygdalina*". Indian Journal of Nanoscience**. 2013**;(2):3–6.
7. Akinpelu D. A. "*Antimicrobial activity of Vernonia amygdalina leaves*". Fitoterapia.

1999;(70):432–434.

8. Farombi E. O and Owoeye O. "*Antioxidative and Chemopreventive Properties of Vernonia amygdalina and Garcinia biflavonoid*". International Journal of Environmental Research and Public Health. **2011**;(8):2533–2555.
9. Francois J., Bonnet R., Bru J., Caron F., Cattoen C. and Cattoir V.." *Comité de l'antibiogramme de la societé francaise de microbiologie*". Société Francaise Microbiologie. **2016**;(1):1-117.
10. Winter CA, Risley EA, Nuss GW. Carrageenin-induced edema in hind paw of the rat as an assay for antiinflammatory drugs. Proceedings of the society for experimental biology and medicine. 1962;111(3):544-7.
11. Belle Ebanda Kedi P, Eya'ane Meva F, Kotsedi L, Nguemfo EL, Zangueu CB, Ntoumba AA, Mohamed HEA, Dongmo AB, Maaza M. Eco-friendly synthesis, characterization, *in vitro* and *in vivo* anti-inflammatory activity of silver nanoparticle-mediated *Selaginella myosurus* aqueous extract. International journal of nanomedicine. 2018;13:8537.
12. CoPath C d P. La réaction inflammatoire. Les inflammations. 2012;
13. Prathna, T.C., Chandrasekaran. N., Raichur. M.A. and Mukherjee. A.. "*Biomimetic synthesis of silver nanoparticles by citris limon (lemon) aqueous extract and theoritical prediction of particle size*". Colloids Surf. B. **2011**;(82): 152-159.
14. Mie, G.,. "*Beitrage zur Optik truber Medien, speziell kolloidaler Metallosungen*". Ann. Phys. **1908**;(330): 345-377.
15. Eya'ane Meva. F, Segnou M L,Okalla Ebongue C, Ntoumba A A., Belle Ebanda Kedi P, Vandi D, Etoh M-A., Mpondo Mpondo E A. "Spectroscopic synthetic optimizations monitoring of silver nanoparticles formation from *Megaphrynium macrostachyum* leaf extract". Brazillian Journal of Pharmacognosy. **2016**;(26):640-646.
16. Mulvaney, P., "*Surface plasmon spectroscopy of nanosized metal particles*". Langmuir **1996**;(12):788-800.
17. Thombre, R., Parekh, F., Lekshminarayanan and P., Francis, G. "*Studies on antibacterial and antifungal activity of silver nanoparticles synthesized using Artocarpus heterophyllus leaf exract*". Biotechnol. Bioinf. Bioeng. **2012**;(2): 632-637.
18. Awwad, A.M., Salem, N.M., Abdeen, A.O. "Green synthesis of silver nanoparticles using carob leaf extract". Adv. Matter Lett. **2013**;(6):726-730.
19. Iravani, S., Zolfaghari, B. "*Green synthesis of silver nanoparticles using Pinus eldarica bark extract*". BioMed Res. Int., http://dx.doi.org/10.1155/2013/639725.

20. Khalil. M.M.H., Ismail. E.H., El-Baghdady. K.Z. and Mohamed. D. "*Green synthesis of silver nanoparticles using Acalyptica indica leaf extracts and its antibacterial activity*". Arab. J. Chem. **2013**;(7): 1131-1139.
21. J. Annamalai and T. Nallamuthu, "Green synthesis of silver nanoparticles: characterization and determination of antibacterial potency," Applied Nanoscience. **2016**;(6):259–265.
22. A. Le, T. T. Le, V. Q. Nguyen et al., "*Powerful colloidal silver nanoparticles for the prevention of gastrointestinal bacterial infections*". Advances in Natural Sciences: Nanoscience and Nanotechnology, vol.3, no.4, ArticleID045007, 2012.
23. G. M. Sulaiman, W. H. Mohammed, T. R. Marzoog, A. A. A. Al-Amiery, A.A.H.Kadhum, and A.B.Mohamad,"*Green synthesis, antimicrobial and cytotoxic effects of silver nanoparticles using Eucalyptus chapmaniana leaves extract*." Asian Pacific Journal of Tropical Biomedicine. **2013**;(3):58–63.
24. Pelgrift R. Y and Friedman A. J. "*Nanotechnology as a therapeutic tool to combat microbial resistanc*e" ☆. Advanced Drug Delivery Reviews. **2013**;(65):1803–1815.
25. Tchangou Njiemou, A. F., Paboudam Gbambie, A., Fannang, S. V., Vayarai Manaoda, A., Gvilava, V., Spieß, A., Gildas, F. N., Nelie A. M. K., Agnes, A. N., Philippe, B. E. K., Bertin, S. E., Francis, N., Jean, Y. S. F., Joel, O. A. M., Mesode, N. A., Armelle, M. H. K., Daniel, A. Y., Geordamie, C., Alex, V. S., Vandi, D., Emmanuel, N. N., Francois, E. M, & Janiak, C. (2022). Antimicrobial properties of Strychnos phaeotricha (Loganiaceae) liana bark secondary metabolites at the interface of nanosilver particles and nanoencapsulation by chitosan transport vehicles. Journal of Nanomaterials, 2022(1), 3491267.
26. Patel MK, Mandavia DR, Patel TK, Barvaliya MJ, Tripathi CB. Evaluation of anti-inflammatory, analgesic, and antipyretic effects of ethanolic extract of *Pedalium murex Linn*. Fruits. African Journal of Traditional, Complementary and Alternative Medicines. 2013;10(4):94-100.
27. Di Rosa M, Giroud JP, Willoughby DA. Studies of the mediators of the acute inflammatory response induced in rats in different sites by carrageenan and turpentine. J Pathol. mai 1971;104(1):15-29.
28. Vinegar R, Truax JF, Selph JL, Johnston PR, Venable AL, McKenzie KK. Pathway to carrageenan-induced inflammation in the hind limb of the rat. In: Federation proceedings. 1987. p. 118-26.
29. Vinegar R, Truax JF, Selph JL, Johnston PR, Venable AL, McKenzie KK. Pathway to carrageenan-induced inflammation in the hind limb of the rat. In: federation proceedings. 1987. p. 118-26.

30. Umukoro S, Ashorobi R. Evaluation of anti-inflammatory and membrane stabilizing property of aqueous leaf extract of Momordica charantia in rats. African Journal of Biomedical research [Internet]. 10 déc 2009 [cité 20 juin 2021];9(2).